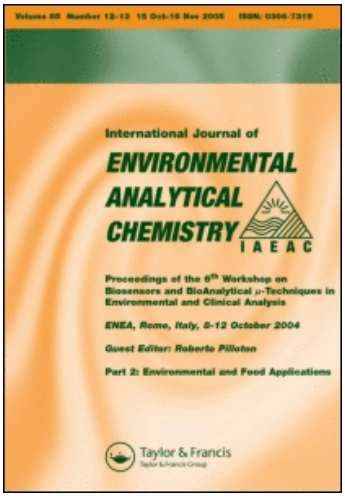

International Journal of Environmental Analytical Chemistry
Publication details, including instructions for authors and subscription information:
http://www.informaworld.com/smpp/title~content=t713640455

In Situ Characterization of Heavy Metal Surface Reactions: The Chromium Case

L. Charlet[a]; A. Manceau[b]
[a] Institut für Anorganische, Analytische und Physikalische Chemie, University of Bern, Bern, Switzerland [b] Laboratoire de Minéralogie-Cristallographie, Universités Paris 6 et 7, CNRS UAO9, Paris, France

To cite this Article Charlet, L. and Manceau, A.(1992) 'In Situ Characterization of Heavy Metal Surface Reactions: The Chromium Case', International Journal of Environmental Analytical Chemistry, 46: 1, 97 — 108
To link to this Article: DOI: 10.1080/03067319208027001
URL: http://dx.doi.org/10.1080/03067319208027001

Intern. J. Environ. Anal. Chem., Vol. 46, pp. 97–108
Reprints available directly from the publisher
Photocopying permitted by license only

IN SITU CHARACTERIZATION OF HEAVY METAL SURFACE REACTIONS: THE CHROMIUM CASE

L. CHARLET

Institut für Anorganische, Analytische und Physikalische Chemie, University of Bern, Freiestrasse 3 3000 Bern, Switzerland

A. MANCEAU

Laboratoire de Minéralogie-Cristallographie, Universités Paris 6 et 7, CNRS UA09, Tour 16, 4 place Jussieu, 75252 Paris, France

(Received 13 March 1991; in final form 2 September 1991)

Mobility and toxicity of heavy metals are largely controlled by chemical reactions which take place at the oxide/water interface. Insights in the mechanisms involved in these reactions can be obtained from the recently developed synchrotron-based fluorescence-yield X-ray absorption spectroscopy. The phenomena investigated in the present study are: the precipitation of Cr(III), its coprecipitation with Fe(III), its sorption onto goethite (αFeOOH), and its oxidation at the surface of a Mn(IV) oxide, birnessite. These examples are used to show how a combination of macroscopic and spectroscopic information provides a mechanistic picture of the mobilization and immobilization pathways of heavy metals in natural systems.

KEY WORDS: EXAFS, surface complexes, adsorption, coprecipitation, reductive dissolution, chromium

INTRODUCTION

The toxicity and mobility of heavy metals present in soil and surface waters depend on their speciation. This speciation arises from the competition among different complexing species for these metal ions. Adsorptive surfaces compete with the dissolved ligands for the system's metal ions, and thus exert a strong control on their speciation, via adsorption, surface precipitation or coprecipitation reactions. These various sorption phenomena are together responsible for the "immobilization" of heavy metals in soils. But mineral surfaces can also catalyze or take part to redox reactions which may then "mobilize" these metals. All these surface processes must be described in detail in order to understand the possible pathways of detoxification of the heavy metals, when present at hazardous concentrations.

Such risk assessments have long been based on information obtained by sequential extraction techniques. More recently, macroscopic models have been developed on

the basis of laboratory macroscopic sorption data to describe quantitatively the surface phenomena responsible of the retardation of a given pollution. Computer code capable of calculating the extent of solute sorption have been coupled with transport model to predict the transport and dispersion of contaminants in surface- and ground-waters. In order to further develop such models, unambiguous information about the stability and molecular structure of species at the colloid/solution interface is required, which can only be obtained with in-situ surface spectroscopy. Invasive and structural spectroscopic methods that require sample desiccation or high vacuum techniques (e.g., electron microscopy and microprobe analysis; X-ray photoelectron (XPS), IR-transmission, IR-ellipsometric, inelastic electron tunneling (IETS), and electron energy loss (EELS) spectroscopies) have contributed significantly to the understanding of adsorbate-surface interactions[1]. Sampling techniques required by these methods often change irreversibly the surface species of interest, and molecular level information about the mechanisms of surface reactions suggested by data obtained with these methods may bear little resemblance to the mechanisms operating in a natural colloidal system.

Recent advances in the development of non-invasive, in-situ spectroscopic techniques have been applied successfully to the study of natural colloids in aqueous suspensions. Among other emerging spectroscopic methods the recently developed X-ray absorption spectroscopy (XAS) is one of the few methods capable of providing direct structural information on dilute heavy metal species sorbed on wet surfaces at room temperature. It shall be used in this study to decipher two key mechanisms involved in the cycle of chromium in soils and surface waters.

CHROMIUM CYCLE IN THE ENVIRONMENT

Chromium is introduced into surface waters as a consequence of the weathering of the rocks such as shales and serpentine[2] and as by-products of steelworks, chromium electroplating, leather tanning and chemical manufacturing industries. These industries produce waste waters rich in Cr(VI) and sludges containing up to 5 g kg^{-1} Cr(III)[3]. Cr(III) and Cr(VI) are the two thermodynamically stable oxidation states in natural waters[4].

Chromium (VI) is the most soluble form of chromium. The chromate and bichromate ions, whose solubility may be controlled by $FeCr_2O_4(s)$[5], are weakly adsorbed on mineral surfaces. For example, the surface complexation constant for chromate ion with an iron oxyhydroxide surface (goethite) are very close to the one obtained for selenate[6,7], an ion whose adsorption on goethite has, in turn, been shown to involve only long range electrostatic forces[8]. Chromium (VI) can therefore easily migrate, and it represents the major form of chromium both dissolved in lake waters[9] and uptaken by plants[10,11].

Chromium (V) is an unstable species which may be responsible for the mutagenic and mammalian carcinogenic properties of chromium. It has been shown by ESR spectroscopy to be stabilized by intracellular organics[11] and by humic acids[12]. Organics are often involved in the reduction of Cr(VI) in acid soils[13,14] and in rivers

and sediments[15]. Other reductants include sulfides, ferrous containing minerals (magnetite[16] and biotite[17]) and free ferrous ion. The latter is widely used in water treatment plants and in analytical chemistry to remove Cr(VI) out of dilute solutions[18], and this reduction occurs also in root cells[19].

Chromium (III) is in the pH range of natural waters the most unsoluble form of chromium. It is extensively hydrolyzed and polymerized[20–22]. The Cr(III) polymers are used in the industry as tanning agent: positively charged, they are bound to the organic groups present at the leather surface[23]. Cr(III) has also a high affinity for mineral surfaces, such as silica[24], aluminum oxides[25] and iron oxides[26]. This "particulate" form of chromium is responsible for a large portion of chromium transported in polluted rivers[27]. Cr(III) is very stable with regard to oxygenation (the oxidation rate constant by O_2 is $0.37\ yr^{-1}$[28]), but it readily converts to Cr(VI) in presence of Mn(III, IV) oxide surfaces[29,30]. In this study we shall explore with X-ray absorption spectroscopic techniques the microscopic mechanisms responsible for the high affinity of Cr(III) for Fe oxyhydroxide surfaces (a cause of its "immobilisation") and the mechanisms involved in the oxidation of Cr(III) by Mn(IV) oxides.

OUTLINE OF THE X-RAY ABSORPTION SPECTROSCOPY

XAS consists in recording the absorption, by a given sample, of X-rays as a function of the wavelength. The spectral scan is performed in the vicinity of an X-ray absorption edge (K or L) of the chosen target element. XAS is therefore a *bulk*, element specific spectroscopic method. Unlike most spectroscopic methods however, *most elements are spectroscopically active.* XAS can therefore be used to study compositionally complex materials, by successively tuning to the absorption edge of each spectroscopically active atom present within the sample.

By convention, XAS spectra are divided in two regions: (1) the X-ray absorption near-edge structure (XANES), in the range from 20 eV below to 70 eV above the absorption edge, and (2) the extended X-ray absorption fine structure (EXAFS) for higher energies, up to 800 eV beyond this edge. The discussion below covers only the highlights of the EXAFS spectroscopy, and the reader is referred to recent monographs for a complete discussion of XAS[31,32].

In the EXAFS regime, photons with an energy larger than the threshold energy are absorbed by the target atom which in turn ejects an ionized photoelectron. The kinetic energy of this electron allows it to reach the three to four first shells of neighboring atoms and to be backscattered by them. Interferences between outgoing and incoming electronic waves influence the probability of absorption of the incident X-ray photon, and hence, the probability of emission of a decay fluorescence photon. These interferences thus modulate the absorption coefficient, which results in the existence of oscillations in the EXAFS spectrum. After subtraction of the background absorption, the EXAFS data are treated by Fourier transform techniques to obtain a radial distribution function (RDF), i.e. a one dimensional representation of the local structure around the absorber atom. The analysis of the RDF provides information on distances, coordination numbers and sometimes, identity of the neighboring

atoms. EXAFS spectroscopy is therefore a particularly valuable tool for the structural characterization of surface complexes. The main features of EXAFS are:

—it yields structural quantitative information extending beyond the first coordination shell, with an accuracy of ± 0.02 Å for distances and $\pm 20\%$ for coordination numbers. This allows to distinguish various sorption mechanisms, as discussed below.

—it works whatever the crystallinity or non-crystallinity of the solid phase, since in any event this method only detects the two or three closest shells of neighbors around the absorbing atom (≤ 5–7 Å).

—it is an in-situ non invasive method which allows systems to be studied in their natural aqueous environment, e.g. as wet paste.

—finally, the high intensity of the X-ray synchrotron radiation combined to the sensitivity of the fluorescence-yield mode (which minimizes matrix absorption effects and maximizes signal-to-noise ratio) allow to study systems with metal concentration down to 0.1% per weight (metal adsorbed per metal in the adsorbent), a concentration to be found in heavily polluted soils and sediments[15].

Sorption of heavy metals may result from various microscopic mechanisms[33]: (1) when the ion is attracted to the surface via long range coulombic forces but retains its water of hydration, it either stands within the diffuse ion swarm, or forms an *outer-sphere complex* with the surface reactive group; (2) when the ion looses some of its hydration water molecules to be directly bound to the surface by short-range forces (chemical bond), it forms with the surface reactive groups an *inner-sphere surface complex*; (3) when this innersphere complex involves sorbed polymers, *surface nucleation*, (and eventually *precipitation*), occurs; finally (4) when the sorbed metal ion is found within the sorbent matrix, *lattice diffusion* or *coprecipitation* has occurred. These different mechanisms are often undistinguishable by macroscopic studies[33], but may be discriminated by EXAFS spectroscopy. The RDF of a metal atom sorbed according to the first mechanism depicts a single peak, that is the oxygen atoms of the hydration water molecules (or in the case of oxyanions, the oxygen atoms of the anion). Selenate ions have been shown to be sorbed on goethite by such a mechanism[8]. On the other hand, the presence in the RDF of additional peaks is indicative of an organized local structure about the target sorbed atom. EXAFS spectroscopy allows unambiguously to distinguish whether a given peak arises from atoms similar to the target atom (an indication that mechanism 3 has occurred), or from other types of atoms (an evidence for mechanism 2 or 4), only if the adsorbed metal and the metal present in the sorbent have significant difference in backscattering amplitude and phase shifts. This condition is fulfilled whenever these atoms have a Z-contrast, i.e. difference in atomic number, greater than about 10. Examples of application include Co^{2+} sorbed on Al_2O_3 and TiO_2[34], SeO_3^{2-} sorbed on goethite[8], and UO_2^{2+} sorbed on hydrous ferric oxide[35,36]. When this condition is not fulfilled, the distinction between sorbate metal atom (e.g. Cr) and metal atoms present in the sorbent (e.g. Fe or Mn) and thus the distinction between mechanisms (2), (3) and (4) is nonetheless feasible, but it is less straightforward and it requires the combination of both spectroscopic and mineralogical data.

This later approach will be followed in the present study, in which the investigated phenomena are: the precipitation of Cr(III), its coprecipitation with Fe(III), its sorption onto goethite (αFeOOH), and its oxidation at the surface of a Mn(IV) oxide, birnessite.

EXPERIMENTAL PROCEDURE

Materials

The methods used to prepare goethite (αFeOOH) and birnessite have been described elsewhere[37,38]. The N_2 BET specific surface area of the two solids are: 19.1 m^2g^{-1} for goethite and 27.0 m^2g^{-1} for birnessite. The structure of goethite is depicted in Figure 1 and that of birnessite in Figure 2. Birnessite is a Mn(IV) phyllomanganate.

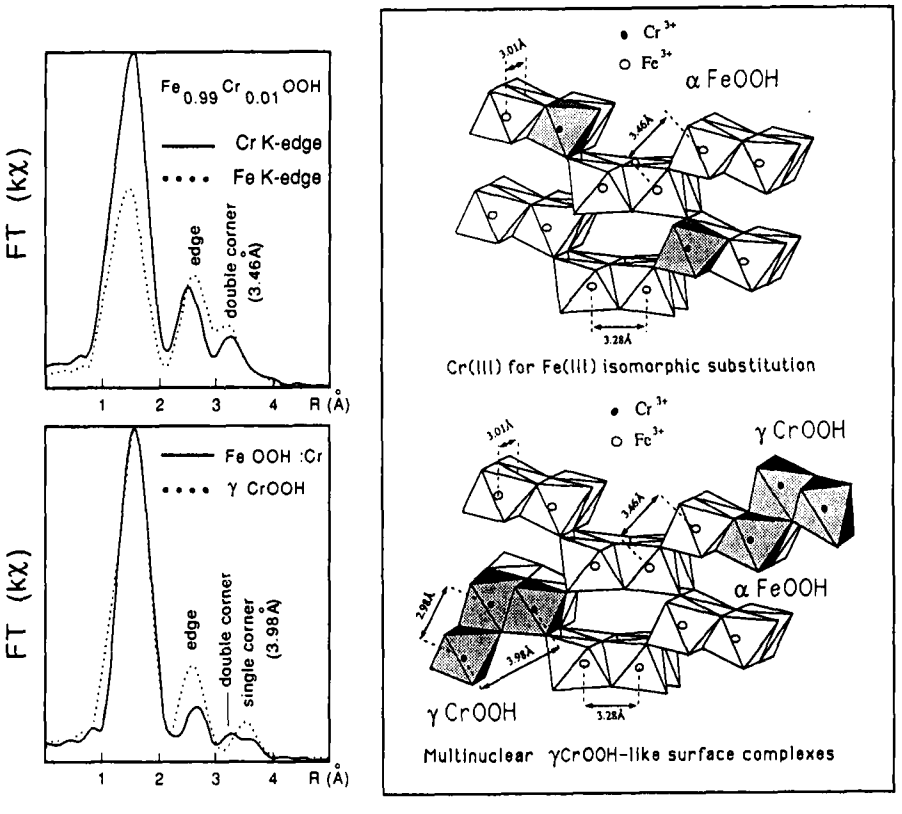

Figure 1 Coprecipitation of Fe(III) and Cr(III) (upper two figures); sorption of Cr(III) onto goethite (lower two figures). Left: EXAFS results, right: structural interpretation.

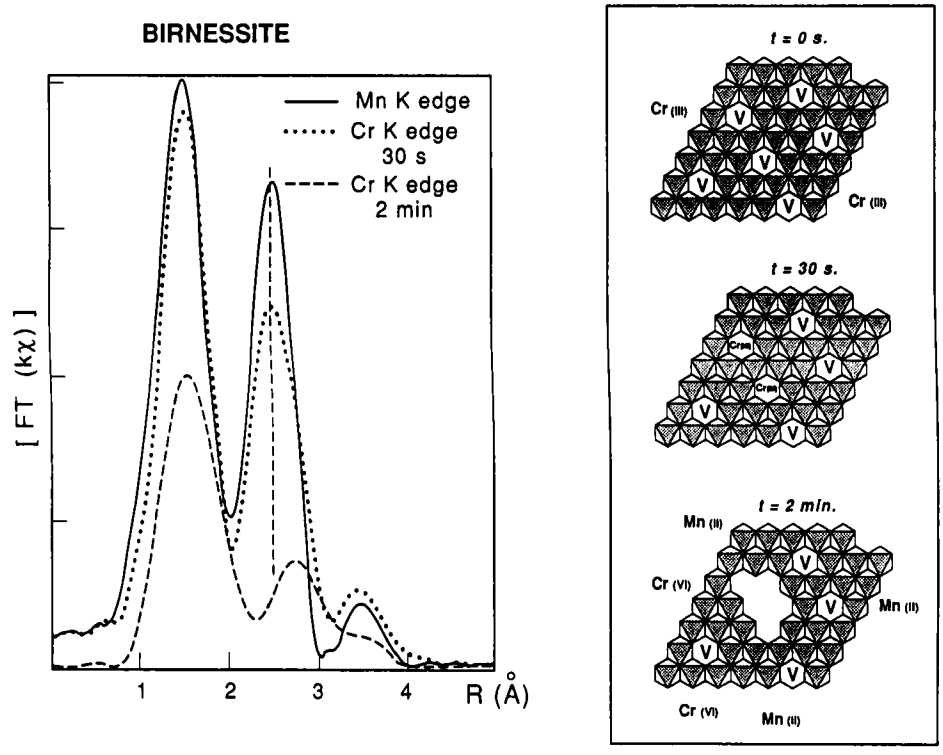

Figure 2 Cr(III) oxidation at the surface of birnessite. Left: EXAFS results, right: structural interpretation of the kinetics.

Within each Mn octahedra layer, one Mn atom out of six is lacking. This creates a deficit of charge and thus a permanent surface charge[39]. The chemical formulae of birnessite is: $(Na^+)_4(Mn_{14}O_{14}^{4-})\cdot(H_2O)_9$[38].

Procedures

Since all previous EXAFS cation adsorption studies have shown the presence of polymers at the mineral/water interface[34,40], the difficulty in such experiments is to control and minimize the formation of these polymers in solution, in order to distinguish what is catalyzed by the surface from what is formed in solution. This is all the more true for chromium(III), which is known to polymerize extensively and slowly in the pH range where sorption occurs[20–22].

Cr(III) sorbed samples were prepared by mixing an aliquot of a 0.6 M NaCl, 10^{-3} N HCl, 0.005 M $CrCl_3$ solution with a 0.6 M NaCl suspension of HFO, whose pH had been previously adjusted at pH 3.00. This suspension was slowly (8 μeq min^{-1}) coulometrically titrated up to pH 4.0. After equilibration for a week at 25.00°C, the suspension was filtered and the filter pad washed with 0.6 M NaCl,

10^{-4} N HCl solution, in order to remove equilibrium entrained solution and non adsorbed Cr(III). Within this procedure, only 1% of the total chromium could have been at the most present as polymer in solution[41]. The surface coverage is equal to 7.5% of a monolayer, assuming a surface site density of 7 sites nm^{-2}.[8]

A different procedure has been followed in the experiments with birnessite, because of the very fast redox kinetics to be studied. In these experiments the Cr solution and the birnessite suspension were separately, coulometrically titrated up to pH 4.00. At $t = 0$ they were mixed together. After equilibration for 30 sec or 2 min, the suspension was filtered and washed, as described above.

Data collection and analysis

All EXAFS data were obtained at the LURE synchrotron french facility (1.85 GeV and 300–260 mA beam current). Cr K-edge spectra were recorded in the fluorescence mode and Fe K-edge spectra in the transmission mode. Fluorescence-yield spectra were collected using a plastic scintillator. Elastic scattering was attenuated with vanadium filters. All spectra were recorded first on wet paste at room temperature, and second at 77 K. Since no change in structural information could be observed, and since spectra recorded at 77 K have a better signal-to-noise ratio, only these spectra will be presented here. The analysis of the EXAFS data using the classical plane-wave formalism is described in detail elsewhere[31,32]. Phase shift and amplitude functions were derived from spectra of the following crystallographic references: α- and γ-FeOOH and birnessite.

RESULTS AND DISCUSSION

Sorption of Cr(III) on goethite

Sequential extraction of a variety of soils have shown that chromium was associated with the citrate-dithionate-extractable portion of these soils, i.e. with their Fe-oxides[2,42]. This has raised a considerable interest for the sorption of chromium by Fe oxides. Chromium (III) adsorption has been shown to occur at low pH and to be nearly completed[26,43] at a pH equal to the first hydrolysis constant of Cr(III), i.e. at pH 4.0[20]. Isotherm performed at this pH have indicated a continuum between adsorbed and surface-precipitated Cr(III)[44], and shown that the solubility of this surface precipitate is similar to the solubility of the pure amorphous $Cr(OH)_3$ ($pK_{so} = 30.0$[21]). On the other hand, when Cr(III) is coprecipitated with Fe(III), the Cr solubility of the product is, even at low Fe content, an order of magnitude lower[45], and the activation energy for the dissolution of the product is much higher than that observed for other metal substituted Fe(III) oxyhydroxides[46]. This coprecipitation is therefore a very efficient removal process. It is commonly used to eliminate Cr(III) out of industrial waste waters. As we shall see now, these differences in removal efficiency have been related by EXAFS spectroscopy to a difference in local structure about Cr(III) atoms[44].

The Cr-edge and Fe-edge RDFs of an aged (Fe,Cr)OOH coprecipitate are shown in Figure 1 (upper left corner). They display three peaks, a first oxygen peak, and two metal-neighbor peaks. This type of Fe-RDF has been shown to be indicative of a goethite-like local structure (Figure 1, upper right corner), the second and third peaks corresponding to Fe octahedra sharing edges and corners, respectively[47]. The identity in distance and relative intensity of the two metal–metal RDF's peaks at the Cr and Fe K-edges points to a similar local structure, i.e. an isomorphic substitution of Cr into the goethite network, as depicted on the upper right corner in Figure 1. This substitution is possible because the Fe and Cr octahedra have similar size and are both found in α-type structures.

The RDF of the XRD-amorphous $Cr(OH)_3$ precipitate is also given in Figure 1 (dotted line, lower left corner). The shift to larger distances of the second metal–metal peak as compared to the one discussed above clearly indicates that the local structure in $Cr(OH)_3$ is no longer α-CrOOH, but rather γ-CrOOH. In this structure, Cr octahedra do not any longer share double corners, but instead a single corner with the neighboring octahedra. This structure is also encountered in polymers formed early in the precipitation of Cr(III), namely the Te isomer of Cr tetramer[48]. Thus the homogeneously precipitated chromium hydroxide has a γ-FeOOH-like structure, whereas the one coprecipitated with Fe(III) had an α-FeOOH-like structure. A difference in structure accounts therefore in the present case, as previously observed in the case of Zn hydroxides[49], for a difference in solubility, and consequently for a difference in removal efficiency between the two precipitation processes.

The Cr-RDF of chromium sorbed onto goethite is given in Figure 1 (full line, lower left corner). It depicts the presence of three peaks, which indicate three types (edge, double corners, single corner) of linkages. Octahedra of sorbed Cr atoms are sharing i) edges with *in average* 1.1 to 1.6 first neighbor metal (Fe or Cr) octahedra, ii) double corners with 0.5 to 0.8 second neighbor atom octahedra, and iii) single corners with 1.2 to 1.9 third neighbor atom octahedra. These high *average* numbers of metal atom neighbors can only be accounted for by the formation of small lepidocrocite-like Cr polymers sorbed on the goethite surface, as indicated in Figure 1 (lower right corner). Therefore, although polymerization was kinetically maintained at a very low level in solution (1% of the total chromium at the most), sorbed Cr(III) is not present as individual ion, but rather as polymer. Surface multinuclear complexes have also been observed in other EXAFS studies, of Co^{2+} and Pb^{2+} sorbed onto Al_2O_3[34,40], and have been suggested by various ESR studies[50,51].

When the Cr concentration is increased, these surface multinuclear complexes act as nuclei for the γ-CrOOH surface precipitation[44]. On the other hand, if it is the sorbent crystal, instead of the surface multinuclear complexes, which keeps on growing, the local structure of these complexes may be fossilized and embedded in the crystal structure of the sorbent. Such multinuclear complexes are then reliques of phenomena which occurred at the time of the sorbent growth. Such structures have been recently described in a Fe-containing diaspore[52] and in a Mn-containing goethite[53]. In the first case, hematite-like clusters are present in the channels of the diaspore structure and bound to the aluminous octahedral chains. In the second case, phyllomanganate clusters are embedded in a goethite structure.

Oxidation of Cr(III) on birnessite

Because of their large surface area and of the high solubility of their metal constitutive ions in their low (+II) oxidation state, Fe(III) and Mn(III, IV) oxides and oxyhydroxides are involved in a variety of surface oxidation reactions coupled with their reductive dissolution[54–56]. Among these reactions, the oxidation of Cr(III) at the surface of Mn(III, IV) oxides has been thoroughly studied, due to toxicity and solubility of the product of the reaction, the chromate ion. This reaction has been shown to be an important pathway for solubilization of the chromium (III) introduced in soils via industrial sludges applied to the field. These studies have consistently shown that the rate of oxidation of Cr(III) into Cr(VI) in presence of Mn oxides is proportional to the amount of Mn oxide present, but is independent on solution parameters such as P_{O_2}, ionic strength, and pH[29,30]. All these observations seem to indicate that the oxidation rate is controlled by the formation of an innersphere complex, except the last one, the independence on pH, which would argue for an outersphere electron transfer[30,57]. EXAFS spectroscopy has been used to decipher the mechanism of this reaction and to show that the first of the two previous mechanistic hypothesis is the correct one when Cr(III) is oxidized at the birnessite/water interface[55].

The Mn-edge RDF of birnessite is given in Figure 2. It is characteristic of a phyllomanganate, where each Mn atom is surrounded first by six oxygen atoms and then by five equidistant Mn atoms. In the two dimensional layer of Mn octahedra, one out of six Mn atoms is laking[38], as depicted on the right hand side of Figure 2. This atom deficit or vacancy (denoted V in Figure 2) is responsible for the permanent charge of birnessite[39]. At $t = 0$, when the birnessite suspension is mixed to the Cr^{3+} solution (both had been previously coulometrically titrated at pH 4.0), the Cr^{3+} cations are first attracted by the negative potential originating from the existence of Mn(IV) vacancies. This phenomenon is similar to cation adsorption by clays such as montmorillonite. These clays present on their surface a negative charges arising from isomorphous substitution in octahedral and tetrahedral sheets[33].

The Cr-edge RDF of the birnessite sample after 30 sec exposure to the Cr(III) solution is given in Figure 2 (dotted line). In this RDF a second intense peak is detected, which did not exist either in the Cr solution RDF or in the Cr polymers RDFs (Figure 1). This peak indicates that sorbed Cr^{3+} is not bound to the surface via an outersphere complex and is not present as Cr hydroxy polymer. Analysis of the first neighbor metal (Me) peak indicates that a Cr–Me distance equal to the Mn–Mn distance within birnessite (see the two RDFs), namely 2.90 Å, and the presence of about 4 Me atoms in the atom shell. These two results can only be accounted for by the *diffusion of Cr(III) within the vacancies* present in this mineral, as depicted in Figure 2 (middle figure on the right hand side), and formation of an innersphere complex. This phenomenon can be compared to the diffusion of K^+ ions into montmorillonite siloxane ditriganal cavities[33].

Ninety seconds later, the Cr-edge RDF of the filtered solid phase has drastically changed (Figure 2, dashed line). The second peak observed in the 30 sec RDF has dropped down: Cr atoms are therefore no more present in the birnessite cavities.

The amplitude of the first peak (Cr—O contribution) has also decreased: the electron transfer has occurred, and 45% of chromium remaining in the filter pad is in the Cr(VI) oxidation state[58]. Oxidized chromium atoms are no longer in an octahedral environment, but present as anions in a tetrahedral coordination (CrO_4^{2-}), and these anions are repelled from the negatively charged birnessite surface. In the case where U^{4+}, instead of Cr^{3+}, is oxidized by MnO_2, it has been shown by isotopic exchange that the oxygen of the reaction product (here UO_2^{2-}), originates indeed from the oxide, and not from water molecules[59]. Information on the other reaction product, namely Mn^{2+}, could not be obtained by the present technique. Oxidation of hydroquinone by MnO_2 have shown, however, that part of the Mn^{2+} could be in a first step readsorbed by the negatively charged surface[60]. Finally, the appearance of a new peak in the 2 mn RDF (Figure 2, dashed line) indicates the formation of polymers. This could have been expected since after $t = 0$ the pH was not controlled any more, and the weathering of birnessite is fast enough at pH 4.0 to drift the pH upward. These polymers are expected to be less reactive since they cannot fit within the Mn(IV) vacancies. They may even physically hinder, together with Mn^{2+}, the diffusion of free Cr^{3+} ions toward these vacancies, and their formation may account for the decrease of oxidation rate observed upon increase of Cr(III) total concentration[30]. In this reaction, birnessite appears to act, because of its lacunar structure, as a molecular sieve for free Cr^{3+} ions. This sieve is particularly efficient due to the 2D structure of birnessite (3D Mn(III, IV) oxides are much less efficient oxidants) and to the similarity of Cr(III) and Mn(IV) ionic radii.

The oxidation of Cr(III) at birnessite can finally be mechanistically sketched as follows (Figure 2, right hand side):

1) an electrostatic attraction of the Cr^{3+} cations toward the negatively charged surface,

2) the diffusion of Cr(III) ions within the Mn(IV) vacancies of the lattice,

3) the electron transfer between chromium and manganese atoms via the oxo bridges, and

4) a release of Cr(VI) in solution.

CONCLUSION AND OUTLOOK

With EXAFS spectroscopy one obtains with a reasonable degree of accuracy the distance and number of atoms present in the first three/four atom shells surrounding a target central heavy metal atom sorbed on a wet surface. This information has been combined with macroscopic and mineralogical data to elucidate the mechanisms involved in Cr(III) surface reactions (a sorption and a redox one) of importance in the environment.

Only a few studies have been yet reported in this field. The present study has shown how the structure of the sorbent and in particular the nature and geometry of the surface functional group may control the availability and speciation of heavy metals in the environment.

This type of study is today limited to systems with metal surface coverage equal to at least about 10% of a surface monolayer. However once, in the next five years, the third generation of higher intensity synchrotron radiation sources will have been commissioned (e.g. the European Synchrotron Radiation Facility in Grenoble, France, and the Advance Photon Source at Argonne National Laboratory, USA), the study of metals present in much lower amount (e.g. natural samples) will be possible. In addition, new developments such as fast EXAFS and dispersive EXAFS will allow real time studies to be performed.

Acknowledgements

L. C. is grateful to Professors H. Sticher (ETH-Zürich) and J. Tarradellas (EPF-Lausanne) for providing the opportunity to present these results at the "Soil Residue Analysis Workshop" in Lausanne, March 11, 1991, and wish to thank the support by the Swiss National Science Foundation (Project: 20-28270.90). A. M. acknowledges supports provided by CNRS/INSU, grants 5.06 (program: "Equipement mi-lourd 1990"), and 90 DBT 1.03 (program "Fleuve et Erosion", contribution 296).

References

1. A. T. Bell and M. L. Hair (Eds.) *Vibrational Spectroscopies for Adsorbed Species* (ACS Symp. Ser. **137**, American Chemical Society, Washington, DC, 1980).
2. H. Sticher, *Mittl. Dtsch. Bodenkundl. Gesellsch.*, **27**, 239–245 (1978).
3. S. J. Dreiss, *Groundwater*, **24**, 312–321 (1986).
4. H. Elderfield, *Earth Planett. Sci. Lett.*, **9**, 10–16 (1970).
5. R. E. Cranston and J. W. Murray, *Limnol. Ocean*, **25**, 1104–1112 (1980).
6. L. S. Balistrieri and T. T. Chao, *Soil Sci. Soc. Am.*, **51**, 1145–1151 (1987).
7. J. A. Davis and J. O. Leckie, *J. Colloid Interf. Sci.*, **74**, 32–43 (1980).
8. K. F. Hayes, A. L. Roe, G. E. Brown Jr., K . O. Hodges, J. O. Leckie and G. A. Parks, *Science*, **238**, 783–786 (1987).
9. C. A. Johnson, *Limnol. Ocean.* (submitted).
10. P. R. Shewry and P. J. Peterson, *J. Exp. Bot.*, **25**, 785–790 (1974).
11. G. Micera and A. Dessi, *J. Inorg. Biochem.*, **34**, 157–166 (1988).
12. D. M. L. Goodgame, P. B. Hayman and D. E. Hathway, *Inorg. Chim. Acta*, **91**, 113–115 (1984).
13. E. E. Cary, W. H. Allaway and O. E. Olson, *J. Agric. Food Chem.*, **25**, 305–309 (1977).
14. R. J. Bartlett and J. M. Kimble, *J. Env. Qual.*, **5**, 383–386 (1976).
15. W. C. Pfeiffer, M. Fiszman, L. Drude de Lacerda, M. van Weerelt and N. Carbonell, *Env. Pollution*, (Series B) **4**, 193–205 (1982).
16. A. F. White in: "*Mineral-Water Interface Geochemistry*" (M. F. Hochella Jr. and A. F. White, Eds., Reviews in Mineralogy, Vol. 23, Mineralogical Soc. of Am., Washington D.C., 1990), pp. 467–510.
17. L. E. Eary and D. Rai, *Amer. J. Sci.*, **289**, 180–213 (1989).
18. R. E. Cranston and J. W. Murray, *Anal. Chim. Acta*, **99**, 275–282 (1978).
19. J. E. Gruber and K. W. Jennette, *Biochem. Biophys. Res. Comm.*, **82**, 700–705 (1978).
20. C. F. Baes and R. E. Mesmer, *The Hydrolysis of Cations* (John Wiley, New York, 1976), 489 pp.
21. D. Rai, B. M. Sass and D. A. Moore, *Inorg. Chem.*, **26**, 345–349 (1987).
22. H. Stunzi and W. Marty, *Inorg. Chem.*, **22**, 2145–2150 (1983).
23. K. H. Gustavson, *The Chemistry of Tanning Processes* (Academic Press Inc., New York, 1956), 381 pp.
24. R. O. James and T. W. Healy, *J. Colloid Interface Sci.*, **40**, 42–51 (1974).
25. B. Wehrli, S. Ibric and W. Stumm, *Colloids Surf.*, **51**, 77–88 (1990).
26. D. A. Dzomback and F. M. M. Morel, *Surface Complexation Modeling: Hydrous Ferric Oxide* (John Wiley, New York, 1990), 393 pp.
27. W. Salomons and U. Förster, *Metals in the Hydrocycle* (Springer-Verlag, 1984), 349 pp.
28. D. C. Schroeder and G. F. Lee, *Water Air Soil Pollut.*, **4**, 355–365 (1975).
29. L. E. Eary and D. Rai, *Env. Sci. Technol.*, **21**, 1187–1193 (1987).
30. C. J. Johnson and A. G. Xyla, *Geochim. Cosmochim. Acta*, **55**, 2861–2866 (1991).

31. D. C. Kronisberger and R. Prins (Eds.), *X-Ray Absorption: Principles, Applications, Techniques of EXAFS, SEXAFS and XANES* (John Wiley, New York, 1988) 673 pp.
32. B. K. Teo, *EXAFS: Basic Principles and Data Analysis*. Inorganic Chemistry Concepts 9 (Springer-Verlag, Berlin, 1986), 349 pp.
33. G. Sposito, *The Surface Chemistry of Soils* (Oxford Univ. Press, Oxford, 1984), 234 pp.
34. G. E. Brown Jr., G. A. Parks and C. J. Chisholm-Brause, *Chimia*, **43**, 248–256 (1989).
35. J. M. Combes, *Evolution de la Structure Locale des Polymères et Gels Ferriques lors de la Cristallisation des Oxydes de Fer. Application au Piègeage de l'Uranium*, Ph.D. Thesis, University of Paris 7, France, 1988.
36. A. Manceau, L. Charlet, M. C. Boisset, B. Didier and L. Spadini, *Applied Clay Min.* (in press).
37. Y. Okuda and T. Harada *United States Patent*, **4, 495**, 164–173 (1985).
38. R. Giovanoli, E. Stähli and W. Feitnecht, *Helv. Chim. Acta*, **53**, 209–220 (1970).
39. D. C. Golden, J. B. Dixon and C. C. Chen, *Clays Clay Minerals*, **34**, 511 (1986).
40. G. E. Brown Jr., G. Calas, G. A. Waychunas and J. Petiau, in: "*Spectroscopic Methods in Mineralogy and Geology*" (F. Hawthorne Ed., Rev. Mineralogy, Vol 18, Mineralogical Soc. of Am., 1988), pp. 431–512.
41. F. P. Rotzinger, H. Stünzi and W. Marty, *Inorg. Chem.*, **25**, 489–495 (1986).
42. U. Schwertmann and M. Latham, *Geoderma*, **39**, 105–123 (1986).
43. S. Amirhaeri, S. Koons, M. Martin and H. Patterson, *Water Res.*, **18**, 87–90 (1984).
44. L. Charlet and A. Manceau, *J. Colloid Interface Sci.* (in press).
45. B. M. Sass and D. Rai, *Inorg. Chem.*, **26**, 2228–2232 (1987).
46. R. Lim-Nunez and R. Gilkes, in: *Proc. Intl. Clay Conf.*, Denver 1985 (L. G. Schultz, H. Van Olphen, F. A. Mumpton, Eds.), pp. 197–204.
47. J. M. Combes, A. Manceau, G. Calas and J. Y. Bottero, *Geochim. Cosmochim. Acta*, **53**, 583–594 (1989).
48. H. Stünzi and W. Marty, *Inorg. Chem.*, **22**, 2145–2150 (1983).
49. P. W. Schindler, in: "*Equilibrium Concepts in Natural Water Systems*" (W. Stumm, Ed., Advances in Chemistry Series 67, American Chem. Soc., Washington D.C., 1967), pp. 196–221.
50. W. F. Bleam and M. B. McBride, *J. Colloid Interface Sci.*, **103**, 124–132 (1985).
51. M. B. McBride, in: "*Interactions at the Soil Colloid–Soil Solution Interface*" (G. H. Bolt *et al.*, Eds, Kluwer Academic Pub., Amsterdam, 1991) pp. 149–175.
52. J. L. Hazemann, A. Manceau, P. Sainctavit and C. Malgrange, *Phys. Chem. Minerals* (in press).
53. A. Manceau, A. I. Gorskhov and V. A. Drits, *Am. Mineralogist* (in press).
54. A. T. Stone and J. J. Morgan, in: "*Aquatic Surface Chemistry*" (W. Stumm Ed., John Wiley, New York, 1987), pp. 221–254.
55. J. G. Hering and W. Stumm. in: "*MineralWater Interface Geochemistry*" (M. F. Hochella Jr. and. A. F. White, Eds., Review in Mineralogy, Vol 23. Mineralogical Soc. of Am., 1990), pp. 427–466.
56. P. Adrian, A. S. Lahaniatis, F. Andreux, M. Mansour, I. Scheunert and K. Korte, *Chemosphere*, **18**, 1599–1609 (1989).
57. B. Wehrli, B. Sulzberger and W. Stumm, *Chem. Geology*, **78**, 167–179 (1989).
58. A. Manceau and L. Charlet, *J. Colloid Interface Sci.* (in press).
59. G. Gordon and H. Taube, *Inorg. Chem.*, **1**, 69–75 (1962).
60. A. T. Stone and H. J. Ulrich, *J. Colloid Interf. Sci.*, **132**, 509–522 (1989).